Journal of the European Ceramic Society 22 (2002) 27–34

www.elsevier.com/locate/jeurceramsoc

Sintering and grain growth of CoO-doped CeO_2 ceramics

Tianshu Zhang [a,*], Peter Hing [a], Haitao Huang [a], J. Kilner [b]

[a] *Advanced Materials Research Centre, Division of Materials Engineering, School of Applied Science, Nanyang Technological University, Nanyang Avenue, Singapore 639798*

[b] *Department of Materials, Imperial College of Science, Technology and Medicine, London SW7 2AZ, UK*

Received 23 August 2000; accepted 16 February 2001

Abstract

Co-doped CeO_2 powders with atomic ratios equal to 0.25, 1 and 3% were synthesized by the conventional mixed-oxide method. No binary compounds were detected in the CeO_2–CoO system, and the Co element exists as the state of Co^{2+} in the samples sintered above 1000°C. A small amount of Co doping reduces sintering temperatures and promotes grain boundary mobility dramatically. Over 99.0% of relative density (R.D.) can be obtained for 0.25% Co-doped sample sintered at 1300°C for 2 h, compared with ~ 96% of relative density for pure CeO_2 sintered at 1525°C for 2 h. The results from grain growth kinetics study indicate that grain growth exponent, n, and activation energy, Q, are 3 and 697 ± 37 kJ/mol for pure CeO_2, 4 and 572 ± 57 kJ/mol for 0.25% Co-doped CeO_2, respectively.

Keywords: CeO_2; CoO doping; Grain growth; Microstructure-final; Sintering

1. Introduction

In recent years, ceria-based materials have been considered as one of the most promising electrolytes for reduced temperature SOFC (solid oxide fuel cell) system due to their high ionic conductivity at moderate temperature.[1–3] Being a highly refractory material, however, ceria based materials are difficult to densify below 1500°C.[4,5] This makes it difficult for the manufacture of ceria-based electrolyte for SOFC system, because ceria-based electrolyte and other components, such as cathode and anode, have to be cofired below 1500°C. In order to reduce the sintering temperature, two methods, either preparing ultrafine CeO_2-based powders or using sintering promoters, have been exploited. For the former case, there is a great volume of literature concerning the preparation of ultrafine CeO_2 powder by chemical and physical methods.[6–10] It is surprising to note, however, that there are only few literature reports concerning the densification of commercial CeO_2 powder by using sintering promoters.[11]

For cost effectiveness, we have used commercial powders as starting materials. A range of potential sintering promoters have been explored to improve the sinterability of commercial CeO_2 powder. Both Fe_2O_3 and MnO_2 are proven to be a good sintering promoter for CeO_2 as found and discussed earlier.[12,13] CoO is chosen in this study as a sintering promoter because it is the neighbor of the above-mentioned two elements. Moreover, based on the effect of severely undersized dopant ions reported by Chen and Chen.[14] The Co^{2+} ion may have the tendency to enhance grain boundary mobility of CeO_2 since its ionic size is much smaller than that of the matrix ion (i.e. Ce^{4+}). To our knowledge, there are not any literature reports concerning the sintering behavior of CeO_2 with CoO as an additive. However, CoO is reported as an effective dopant for the densification of SnO_2.[15,16] Varela et al.[15] and Cerri et al.[16] reported that addition of 0.5 to 2 mol% CoO into SnO_2 promotes the densification of this oxide up to ~ 99.0% of the theoretical density; and the sintering of Co-doped SnO_2 seems to be controlled by solid state diffusion because of the absence of experimental evidence for an eutectic liquid in this system. They deduced that Co^{2+} ions incorporating into SnO_2 crystallites acts as an acceptor leading to the addition of oxygen vacancies in SnO_2, thus enhances the densification rate of this oxide.

Recently, we have found that a small amount of Co doping promotes the densification of commercial CeO_2 powder remarkably. The effect of Co doping on the

* Corresponding author.
E-mail address: p142713729@ntu.edu.sg (T. Zhang).

0955-2219/01/$ - see front matter
PII: S0955-2219(01)00240-0

sintering behavior and microstructural evolution is presented in this study for Co-doped CeO_2 during the non-isothermal and isothermal sintering. Moreover, the grain growth kinetics of undoped and 0.25% Co-doped CeO_2 is also carried out using the well-known grain growth model.[17]

2. Experimental

2.1. Sample preparation

Commercial CeO_2 (>99.9% in purity) and $CoSO_4$ (>99.0% in purity) were used as starting materials. Co-doped CeO_2 powders with atomic ratios equal to 0.25, 1 and 3% were synthesized by the conventional mixed-oxide method. The powders were ground in ethanol by ball-milling for over 24 h and dried. After being calcined at 800°C for 0.5 h, the samples were ball-milled again for over 24 h. The mixtures were pressed at about 50 MPa into pellets using a die with 10 mm diameter. Green densities are about 60% of theoretical. In order to confirm whether there are any solid reactions between CeO_2 and CoO, the sample with Co/Ce atomic ratio of 1.0 was prepared in the same way.

2.2. Sintering experiment

Conventional, pressureless sintering studies were performed in a vertical dilatometer (System 16/18, Setaram, France) or a furnace. The dilatometer allows continuous monitoring of axial shrinkage. Two sets of sintering schedules were used, i.e. constant-heating-rate (CHR) sintering and isothermal sintering. During the CHR experiments, the samples were heated at a constant rate of 10 K/min to a desired temperature and then cooled to room temperature. Isothermal sintering was conducted in the temperature range of 1300–1550°C. The samples were heated up to a desired temperature at a heating rate of 15 K/min and then held at this temperature for 1–3 h, after that the samples were cooled to room temperature.

The isotropic shrinkage of the samples was confirmed by measuring the lateral and axial shrinkage. The time-dependent density, ρ, therefore, was calculated from the following equation:[18]

$$\rho = \left(\frac{L_f}{L_t}\right)^3 \rho_f \quad (1)$$

where L_f is the final length of the sample, L_t is the time-dependent length equal to the value of $(L_0 - \Delta L_t)$ (L_0 is the original length of the sample and ΔL_t is the displacement of the sample at a certain time, t) and ρ_f is the final density obtained from the mass and dimension of the sample.

2.3. Characterization of samples

The raw powder with Co/Ce = 1.0 was measured using thermal gravimetric and differential thermal analysis (TG-DTA). The phase identification of samples, after each heat treatment at 1200–1600°C, was performed using X-ray diffraction (XRD) with CuK_α radiation. Densities of sintered pellets were measured using both Archimede's method with water or calculated from the mass and the dimensions of the samples. It was found that both the methods provide almost the same value. Microstructure of the samples, i.e. well-polished surface after thermal etching, was observed using scanning electron microscopy (SEM). Grain sizes were measured from SEM micrographs of the etched samples by the linear intercept technique described by Mendelson.[19] The average grain size, D, was obtained as follows: $D = 1.56\ L$, where L is the average grain-boundary intercept length of a series of random lines on the SEM micrographs.

3. Results and discussion

3.1. Phase evolution

The decomposition of $CoSO_4$ into Co_2O_3 takes place below 750°C.[20] In our case, after calcination at 800°C for 1 h, the powder with Co/Ce = 1 should consist of CeO_2 and Co_2O_3. This sample was investigated using TG-DTA at a heating rate of 10 K/min in the temperature range of room temperature to 1400°C in air, and the result is shown in Fig. 1. An exothermal peak on the

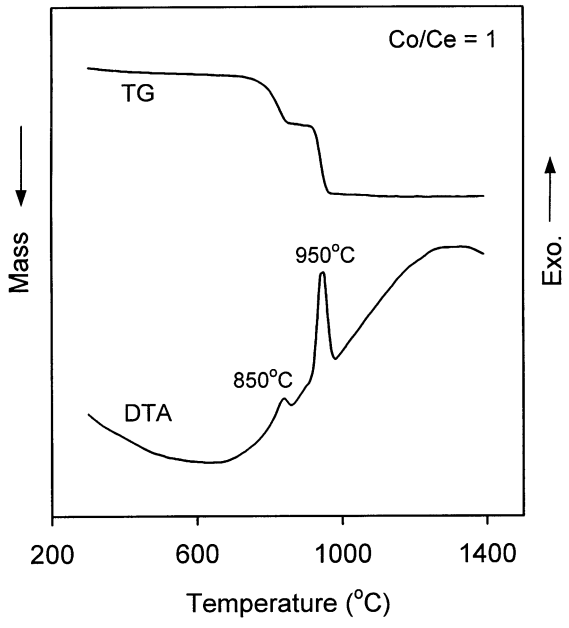

Fig. 1. TG-DTA curves of the sample with Co/Ce = 1.0 sintered at a heating rate of 10 K/min to 1450°C in air.

DTA curve at 850°C with a mass loss can be attributed to the transition of Co_2O_3 into Co_3O_4,[16] i.e.

$$3\ Co_2O_3 \xrightarrow{850^\circ C} 2\ Co_3O_4 + 1/2\ O_2 \uparrow \quad (2)$$

When temperature is up to 950°C, another exothermic peak and its counterpart, i.e. mass loss, can be observed on the DTA and TG curves. It is attributed to the following reaction:

$$2\ Co_3O_4 \xrightarrow{950^\circ C} 6\ CoO + O_2 \uparrow \quad (3)$$

Above 1000°C, no any change can be found on both the DTA and TG curves. It means that Co element exists in the state of Co^{2+} in the sample sintered above 1000°C. This result is in good agreement with that from XRD measurement. As shown in Fig. 2, only two crystalline phases, i.e. CeO_2 and CoO, can be detected in the sample (with Co/Ce = 1.0) sintered at 1400°C, which suggests that no solid-state reaction occurs between CeO_2 and CoO. This is also in agreement with the report by Dontsov et al.[21]

3.2. Non-isothermal sintering

Fig. 3 shows the linear shrinkage rate ($d(\Delta L/L_o)/dt$) as a function of temperature for different Co contents. 1% Co-doped sample exhibits a similar shrinkage trend to that of 0.25% Co-doped CeO_2. For clarity, the curve for 1% Co doping is omitted. It is observed from this figure that the addition of Co shifts somewhat the onset of sintering towards lower temperatures; moreover, the small amount of Co doping decreases the temperature of maximum shrinkage rate (T_{max}) remarkably. For example, T_{max} decreases from 1428°C for pure CeO_2 to 1214°C for 0.25% Co-doped CeO_2. The difference in the values of T_{max} for both the samples is more than 200°C. These results suggest that 0.25% Co doping reduces the sintering temperatures by over 200°C. Contrary to the action of Fe_2O_3 or MnO_2 doping on CeO_2,[12,22] however, it can be seen that the values of T_{max} decreases as the doping level increases in the whole Co content used. It may be due to the effect of trapped pores along grain boundaries and in grain interiors as shown below.

The relative density as a function of temperature for different Co contents is shown in Fig. 4. In the temperature range used (from room temperature to 1550°C), the density of pure CeO_2 increases as the temperature increases. Pure CeO_2 has only about 92% of relative density at 1550°C. This sintering behavior is very similar to those reported by Zhou et al.[23] Upon adding Co into CeO_2, however, the sintering behavior changes greatly. 0.25% Co-doped sample has ~92% R.D. at ~1300°C, and reaches almost full densification (> 99.0% R.D.) at ~1450°C. It is observed from this figure, on the other hand, that with increasing Co contents the densification behavior becomes detrimental. For example, 3% Co-doped sample has only ~97.5% R.D. (at 1550°C), compared with over 99.0% R.D. of 0.25% Co-doped CeO_2 sintered under the same condition.

The effect of Co doping level on grain size and sintered density of CeO_2 ceramic is shown in Fig. 5. It can be seen from this figure that a small amount of Co doping rapidly increases in both the grain size and sintered density. 0.25% Co-doped sample provides maximum

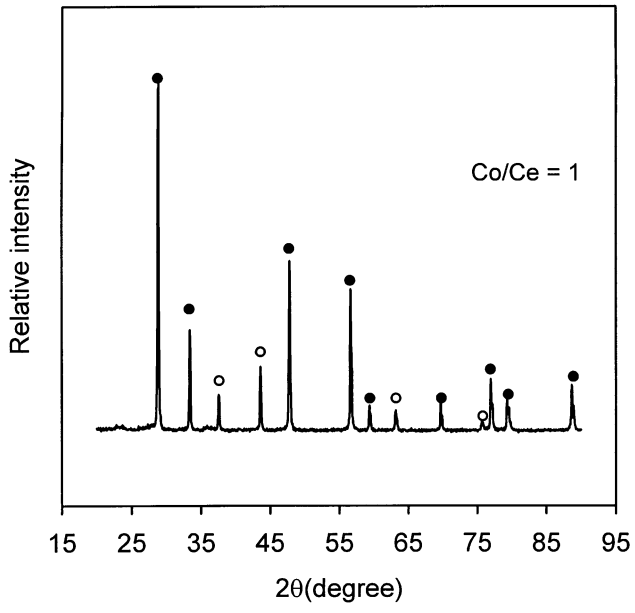

Fig. 2. XRD pattern of the sample with Co/Ce = 1.0 sintered at 1400°C for 5 h in air (●: CeO_2, ○: CoO).

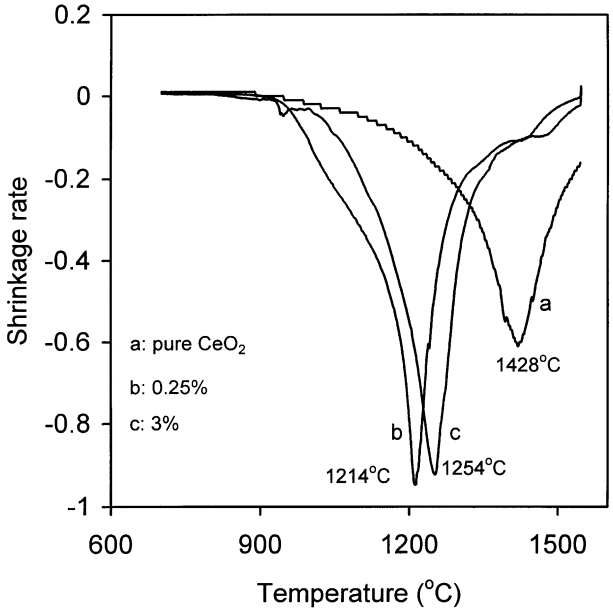

Fig. 3. Shrinkage rate against sintering temperature for (a): pure CeO_2, (b): 0.25% and (c): 3.0% Co-doped CeO_2 sintered at a heating rate of 10 K/min.

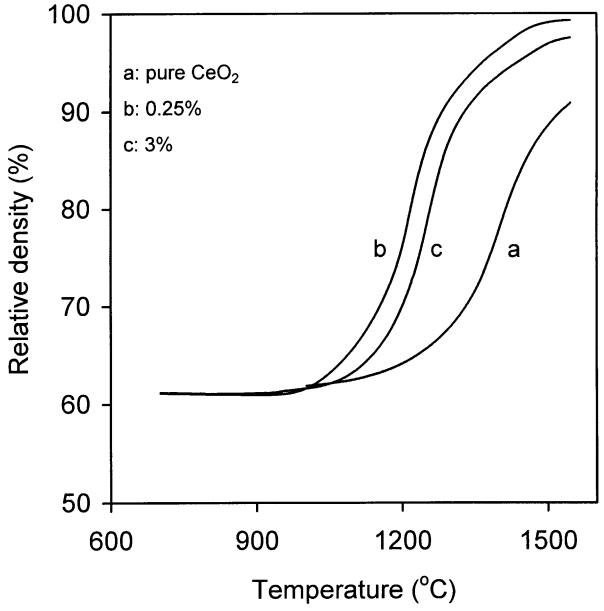

Fig. 4. Relative density vs temperature for (a): pure CeO_2, (b): 0.25% and (c): 3.0% Co-doped CeO_2 sintered at a heating rate of 10 K/min to 1550°C.

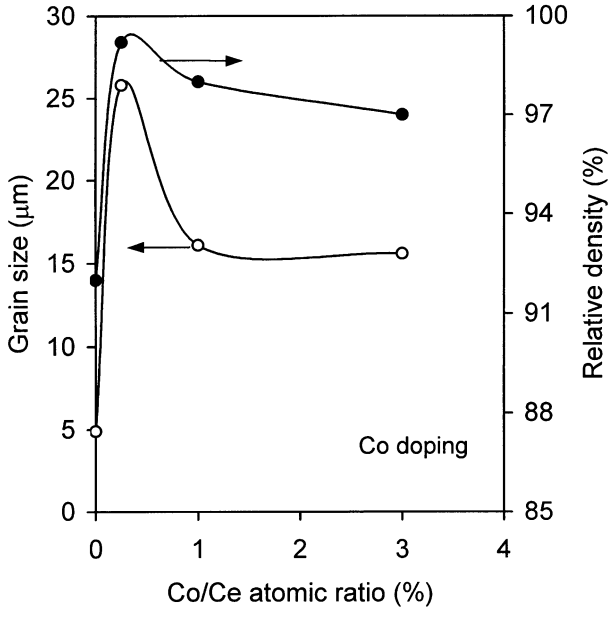

Fig. 5. Effect of Co/Ce atomic ratios on grain size and density of samples sintered at a heating rate of 10 K/min to 1550°C in air.

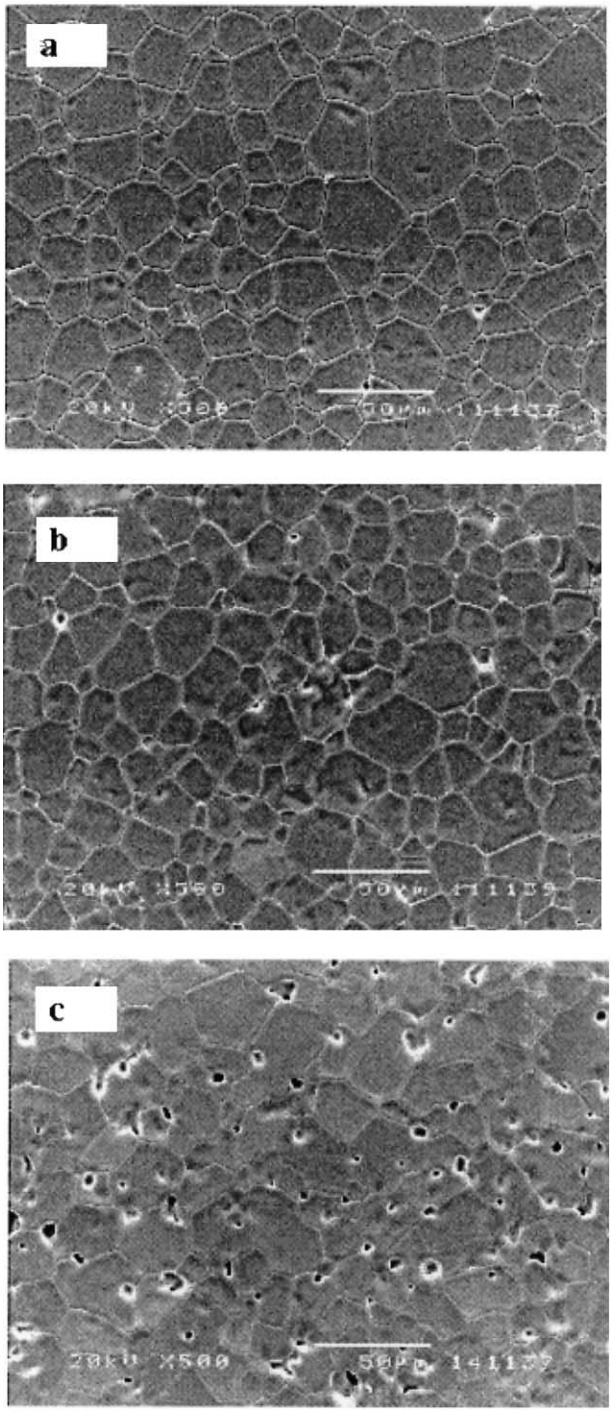

Fig. 6. SEM micrographs of (a): 0.25, (b): 1.0 and (c): 3.0% Co-doped CeO_2 sintered at a heating rate of 10 K/min to 1550°C in air.

values in both the grain size and density. However, further increase in Co doping level leads to a decrease in sintered density. Moreover, unlike the effect of MnO_2 on the sintering of CeO_2[13] where the grain size of CeO_2 increases with increasing Mn doping level, the grain size remains almost unchanged over the Co doping level from 1.0 to 3.0%. Selected micrographs, as shown in Fig. 6, indicate: (1) that the samples with 0.25 and 1.0% Co doping are very dense since practically little or no pores are trapped in the grain interiors as shown in Fig. 6a and b; and (2) that in 3% Co-doped CeO_2 (Fig. 6c) there are many trapped pores along grain boundaries and in grain interior, although this sample has almost the same grain size as that of 1% Co-doped sample. Trapped pores in 3% Co-doped CeO_2 present an interesting phenomenon, that they affect only the

sintered density, but not the grain size. The above result also suggests that high doping level is detrimental for densification.

3.3. Isothermal sintering

Isothermal sintering experiments were conducted using a dilatometer to study the effect of sintering time and temperature on the densification of pure and 0.25% Co-doped CeO_2. In order to avoid the completion of the most densification during temperature ramp, a higher heating rate of 15 K/min was used. The results are shown in Fig. 7. At 1300°C the densification rate of undoped CeO_2 is very slow, and this sample provides only 87% R.D. after 2 h. However, 0.25% Co-doped sample exhibits a very fast densification rate, and at 1300°C over 99.0% R.D. can be reached after 2 h. This density exceeds even that of pure CeO_2 sintered at 1525°C for 2 h. Fig. 8 shows the effect of sintering temperature and time on the microstructure of undoped and 0.25% Co-doped samples. Undoped CeO_2 sintered at 1300°C (Fig. 8 a) is very porous, the grain size is around 0.7 μm, which is slightly larger than that of raw powder (0.4 μm). The sample with 0.25% Co doping sintered at 1300°C (Fig. 8 b) is much denser, and has a larger grain size (~11.7 μm) than that of undoped CeO_2 sintered at 1525°C (~5.3 μm). These results indicate that the small amount of Co doping accelerates the densification rate remarkably and promotes grain boundary mobility.

No evidence is available that a eutectic liquid phase exists in the CoO–CeO_2 system. In addition, as shown in Fig. 1, thermal analysis (TG-DTA) of the sample with Co/Ce = 1.0 up to 1450°C does not display the presence of any endothermic reactions related to liquid-phase formation. This suggests that a fast densification rate in Co-doped samples is not related to liquid-phase sintering. Dontsov et al.[21] studied the phase change in the ternary CeO_2–ZrO_2–CoO system. They pointed out that the dissolution of Co^{2+} into CeO_2 in either substitution sites or interstitial sites depended on the doping level, and Co^{2+} ions resided mainly in the substitution sites

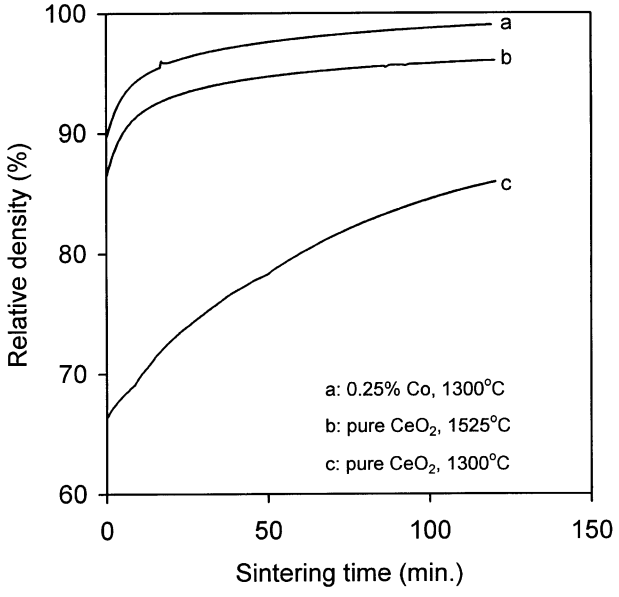

Fig. 7. Effect of sintering time and temperature on the density of undoped and 0.25% Co-doped CeO_2.

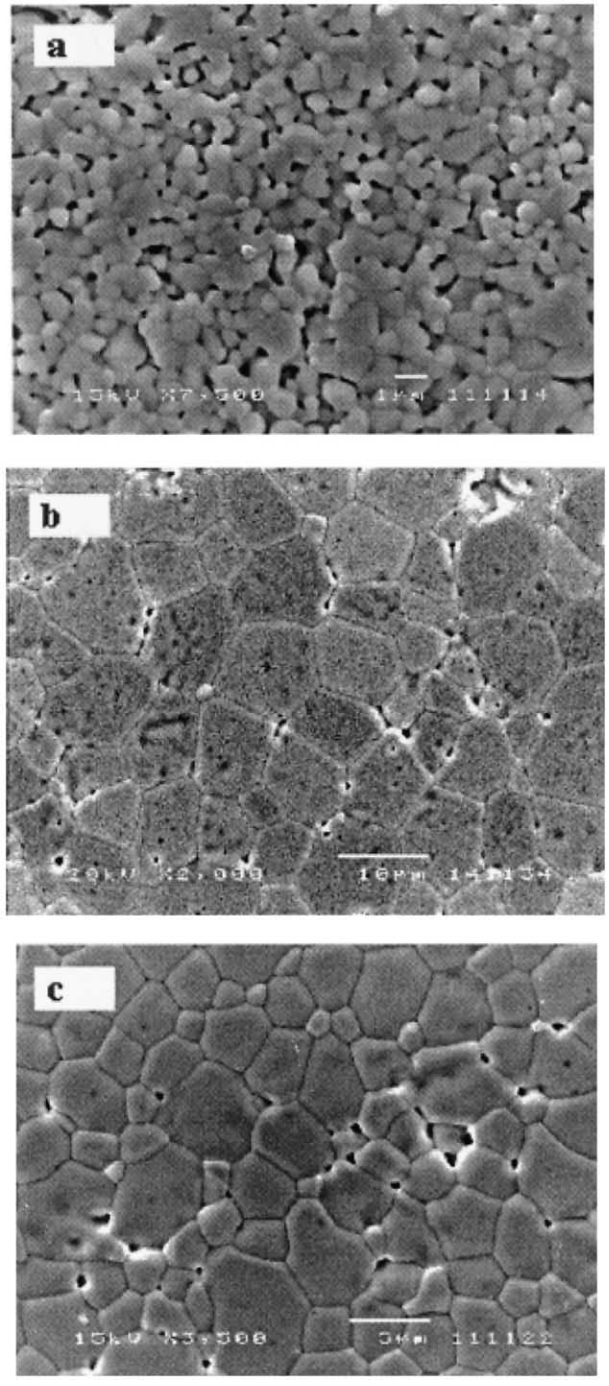

Fig. 8. SEM micrographs of (a): pure CeO_2 and (b): 0.25% Co-doped CeO_2 sintered at 1300°C for 2 h, and (c): pure CeO_2 sintered at 1525°C for 2 h.

when the doping level was less than 5%. In our case, therefore, Co^{2+} ions should be incorporated into Ce^{4+} sites in the CeO_2 crystallites. The substitution reaction can be described using Kroger–Vink notation:

$$CoO \xrightarrow{CeO_2} Co''_{Ce} + Vo^{\bullet\bullet} + Oo^{\times} \quad (4)$$

It seems that we should attribute the quick densification and rapid grain boundary mobility to the formation of oxygen vacancies in Co-doped CeO_2. In fact, this understanding is superficial due to the following reasons. It is well-known that part of CeO_2 is readily reduced to Ce_2O_3 at a high temperature. For example, the concentration of Ce^{3+} is between 0.2 and 0.8% in the temperature range of 1270 to 1420°C.[14] This implies that in undoped CeO_2 there exists a large amount of $Vo^{\bullet\bullet}$ due to the following reaction:

$$Ce_2O_3 \xrightarrow{CeO_2} 2Ce'_{Ce} + Vo^{\bullet\bullet} + 3Oo^{\times} \quad (5)$$

where Ce'_{Ce} indicates one Ce^{4+} site occupied by one Ce^{3+} ion. Moreover, oxygen diffusion is very fast in these fluorite-type oxides such as ZrO_2 and CeO_2. Hence, cation diffusion must be the rate-limiting step for mass transportation. Chen and Chen[14] believe that the diffusion of interstitial Ce is rate-limiting step based on both theoretical consideration and experimental study. Therefore, the incorporation of Co^{2+} into Ce^{4+} sites does not fully account for the quick densification and rapid grain boundary mobility.

By analogy, the sintering behavior of Co-doped CeO_2 should be similar to that of Fe or Mn-doped samples from the periodic properties of elements. As stated above, Fe_2O_3 and MnO_2 are very effective sintering promoters for the sintering of CeO_2. Both the dopants lead to a very fast densification rate of CeO_2. It was found that either Fe or Mn doping changes the early-stage sintering mechanism of CeO_2.[22,24] For example, pure CeO_2 is volume-diffusion controlled sintering, while Fe-doped CeO_2 exhibits viscous flow mechanism.[24] Moreover, severely undersized Fe^{3+} or Mn^{2+} ions promote grain boundary mobility during the final-stage sintering. For the Co doping action, therefore, it is reasonable to assume that Co doping may change the early-stage sintering mechanism of CeO_2; and Co^{2+} ions exhibit the effect of severely undersized dopant because Co^{2+} ion has much smaller size compared with that of Ce^{4+} ion. Co^{2+} ions can enhance grain boundary mobility due to the large distortion of the surrounding lattice that facilitates defect migration of the matrix (i.e. CeO_2).[14]

It is well known that the microstructural evolution of a material can usually be described using grain size and size distribution. The grain growth depends on sintering temperatures and time, which can be analyzed by well-known grain growth kinetics equation,[17] i.e.

$$D^n - D_o^n = Kt \quad (6)$$

and

$$K = K_o \exp\left(\frac{-Q}{RT}\right) \quad (7)$$

where D is the average grain size at time, t, D_o is the average grain size at time, $t=0$, n is the growth exponent, K is a rate constant, K_o is a pre-exponential constant, Q is the activation energy of grain growth, R and T have the common meaning. When D_o is significantly smaller than D, D_o^n can be neglected relative to D^n. Eq.(6) can be simplified as follows:

$$D^n = K_o \exp\left(\frac{-Q}{RT}\right) t \quad (8)$$

The natural logarithmic form of Eq. (8):

$$n\ln D = \ln t - \frac{Q}{RT} + \ln K_o \quad (9)$$

In a proper temperature range, the activation energy, Q, is a constant. So the exponent, n, can be determined from the slope of the plot of $\ln(D)$ versus $\ln(t)$. Subsequently the activation energy, Q, can be obtained from the slope of an Arrhenious plot of $\ln(D^n/t)$ versus $1/T$, based on Eq. (9). In the present study, undoped and 0.25% Co-doped samples were used to study grain growth kinetics. The sintering temperatures were chosen at equal increments: 1350, 1400, 1450 and 1500°C, and for each sintering temperature, four sintering times, i.e. 1, 3, 5 and 8 h, were used.

Fig. 9 shows the plot of $\ln(D)$ versus $\ln(t)$ for undoped and 0.25% Co-doped CeO_2. It can be seen that undoped CeO_2 has the grain growth exponent, n, of ~ 3, while n-value of 0.25% Co-doped CeO_2 is around 4. Based on Eq.(8), we calculated the activation energy, Q, for both the samples, and the results are shown in Fig. 10. Compared with undoped CeO_2, Co doping indeed reduces the activation energy for grain growth of CeO_2, which may be used to explain why Co doping leads to a rapid grain growth.

Chen and Chen[14] found a parabolic grain growth for CeO_2 doped with different dopants. They did not do an activation analysis for doped CeO_2. Their result concerning pure CeO_2 along with the present results in this study are listed in Table 1 for comparison. In our case, both activation energy and growth exponent for pure CeO_2 are higher than their value. It may be due to their starting powder prepared by chemical method. Type of these powders usually has very high reactivity and sinterability. It can be observed that the activation energy for CoO-doped CeO_2 is similar to their undoped value.

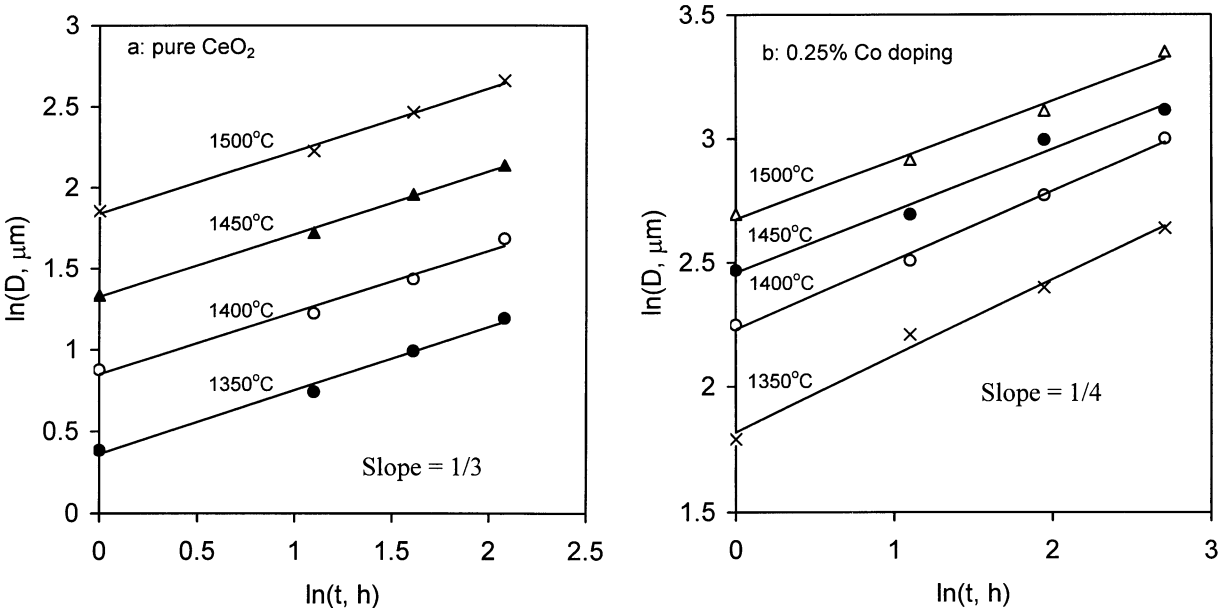

Fig. 9. The plots of $\ln(D)$ versus $\ln(t)$ for (a): undoped and (b): 0.25% Co-doped CeO_2.

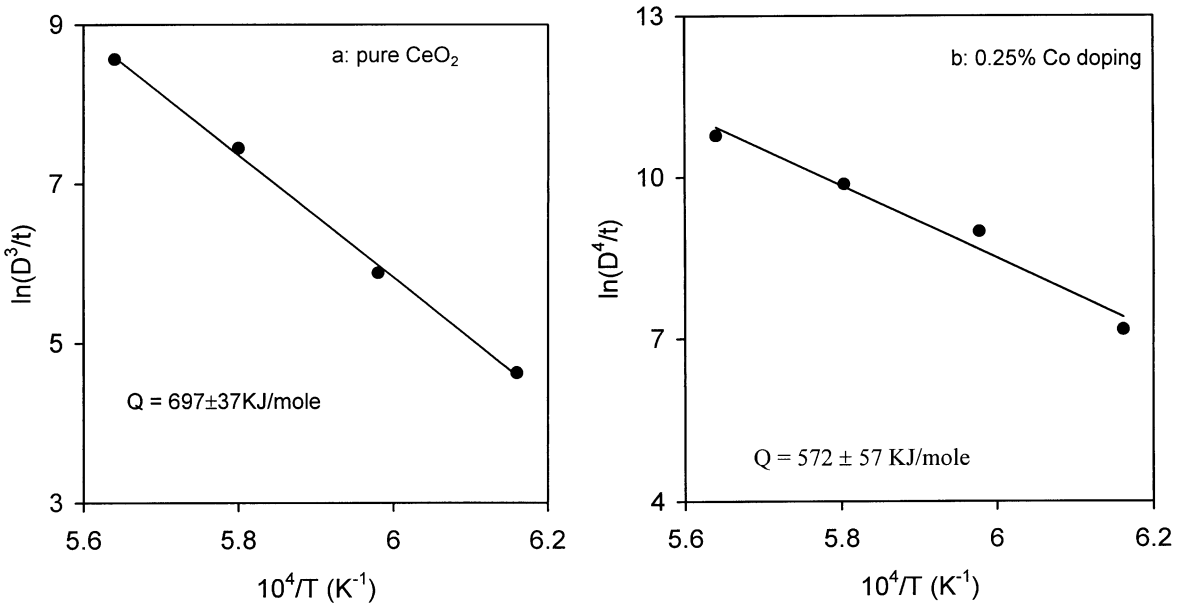

Fig. 10. The plots of $\ln(D^n)$ versus $1/T$ for the calculation of activation energy (Q) for (a): undoped and (b): 0.25% Co-doped CeO_2.

Table 1
Growth exponent, n, and activation energy, Q, of CeO_2-based materials

Researcher	Composition	n-Value	Q (kJ/mol)
Chen and Chen[14]	Pure CeO_2	2	581
This study	Pure CeO_2	3	697±37
	0.25% Co	4	572±57

This further confirms that CoO doping promotes the sinterability of commercial CeO_2.

4. Conclusions

A small amount of Co doping (less than 1% atomic ratio) strongly enhances the densification rate and promotes the grain boundary mobility of commercial CeO_2,

which may be attributed to the change in early-stage sintering mechanisms of CeO_2 due to the addition of CoO as well as the effect of severely undersized dopants.

0.25% Co-doping reduces sintering temperatures by over 200°C. The sample with 0.25% Co-doping reaches maximum values in both the grain size and density compared with other doping levels. However, a high doping level is detrimental for the densification. It is found that in 3% Co-doped sample there are many trapped pores along grain boundaries as well as in grain interiors. Based on the grain growth kinetics study, we found that the samples with low doping levels ($< 1\%$) have a smaller activation energy for grain growth than that of undoped commercial CeO_2. It may further support that Co doping leads to a fast grain growth.

References

1. Inada, H. and Tagawa, H., Ceria-based solid electrolytes. *Solid State Ionics*, 1996, **83**, 1–16.
2. Herle, J.Van, Horita, T., Kawada, T., Sakai, N., Yakokawa, H. and Dokiya, M., Low temperature fabrication of (Y, Gd, Sm)-doped ceria electrolyte. *Solid State Ionics*, 1996, **86–88**, 1255–1258.
3. Zheng, K., Steele, B. C. H., Sahibzada, M. and Metcalfe, I. S., Solid state fuel cells on $Ce(Gd)O_{2-x}$ electrolytes. *Solid State Ionics*, 1996, **86-88**, 1241–1248.
4. Panhans, M. A. and Blumenthal, R. N., A thermodynamic and electrical conductivity study of nonstoichiometric cerium dioxide. *Solid State Ionics*, 1993, **60**(4), 279–298.
5. Zhen, Y. S., Milne, S. J. and Brook, R. J., Oxygen ion conduction in CeO_2 ceramics simultaneously doped with Gd_2O_3 and Y_2O_3. *Sci. Ceram*., 1988, **14**, 1025–1030.
6. Chen, P.-L. and Chen, I.-W., Reactive cerium (IV) oxide powders by the homogeneous precipitation method. *J. Am. Ceram. Soc*., 1993, **76**(6), 1577–1583.
7. Chen, C. C., Nasrallah, M. M. and Anderson, H. U., Synthesis and characterization of $(CeO_2)_{0.8}$,$SmO_{1.5})_{0.2}$ thin films from polymeric precursors. *J. Electrochem. Soc*., 1993, **140**(12), 3555–3560.
8. Zhu, Y. C. and Rahaman, M. N., Hydrothermal synthesis and sintering of ultrafine CeO_2 powders. *J. Mater. Res*., 1993, **8**(7), 1680–1686.
9. Guillpu, N., Nistor, L. C., Fuess, H. and Haha, H., Microstructure study of nanocrystalline CeO_2 produced by gas condensation. *Nanostructured Mater*., 1997, **8**(5), 545–557.
10. Overs, A. and Riess, J., Properties of the solid electrolyte gadolinia-doped ceria prepared by thermal decomposition of mixed cerium-gadolinium oxalate. *J. Am. Ceram. Soc*., 1982, **65**(12), 606–609.
11. Yoshida, H., Miura, K., Fujita, J. and Inagaki, T., Effect of gallia addition on the sintering behavior of samaria-doped ceria. *J. Am. Ceram. Soc*., 1999, **82**(1), 219–221.
12. Zhang Tianshu, Peter Hing, Haitao Huang and Kilner, J., *J. Mater. Processing Technology,* in press.
13. Zhang Tianshu, Peter Hing, Haitao Huang and Kilner, J., Submitted to *J. Mater. Sci. Lett*.
14. Chen, P. L. and Chen, I., Wei, Grain growth in CeO_2: dopant effects, defect mechanism, and solute drag. *J. Am. Ceram. Soc*., 1996, **79**(7), 1793–1800.
15. Varela, J. A., Cerri, J. A., Leite, E. R., Longo, E., Shamsuzzoha, M. and Bradt, R. C., Microstructural evolution during sintering of CoO doped SnO_2 ceramics. *Ceram. Inter*., 1999, **25**, 253–256.
16. Cerri, J. A., Leite, E. R., Gouvea, D., Longo, E. and Varela, J. A., Effect of cobalt (II) oxide and manganese (IV) oxide on sintering of Tin (IV) oxide. *J. Am. Ceram. Soc*., 1996, **79**(3), 799–804.
17. Dutta, S. K. and Sprigge, R. M., Grain growth in fully dense ZnO. *J. Am. Ceram. Soc*., 1970, **53**(1), 61–62.
18. Wang, J. and Raj, R., Estimate of the activation energies for boundary diffusion from rate-controlled sintering of pure alumina doped with zirconia or titania. *J. Am. Ceram. Soc*., 1990, **73**(5), 1172–1175.
19. Mendelson, M. I., Average grain size in polycrystalline ceramics. *J. Am. Ceram. Soc*., 1967, **52**(8), 443–446.
20. Weast, R. C., CRC Handbook of Chemistry and Physics, CRC Press, 1983/1984.
21. Dontsov, G., Vitter, G. and Deportes, C., Etude de la phase fluoritique dans le systeme CeO_2–ZrO_2–CoO. *Re. Int. Hautes Temper. Et Refract*., 1972, **9**, 147–152.
22. Zhang Tianshu, Peter Hing, Haitao Huang and Kilner, J., *Mater. Sci. Eng.B,* in press.
23. Zhou, Y. and Rahaman, M. N., Effect of redox reaction on the sintering behavior of cerium oxide. *Acta. Mater*., 1997, **45**(9), 3635–3639.
24. Zhang Tianshu, Peter Hing, Haitao Huang and Kilner, J., Submitted to *J. Mater. Sci.*